Magnetostratigraphy and palaeoclimate of Red Clay sequences from Chinese Loess Plateau*

SUN Donghuai (孙东怀), LIU Dongsheng (LIU Tungsheng 刘东生)**,
CHEN Mingyang (陈明扬)**, AN Zhisheng (安芷生)
(Xi'an Laboratory of Loess and Quaternary Geology, Chinese Academy of Sciences, Xi'an 710054, China)
and John Shaw
(Geomagnetism Laboratory, University of Liverpool, Liverpool L69 7ZE, UK)

Received March 12, 1997

Abstract Two Red Clay profiles near Xi'an and Xifeng were investigated in an attempt to determine magnetostratigraphic and palaeoclimatic records. The results show that aeolian dust accumulation and the related East Asia palaeomonsoon system had begun by 6.5 Ma, and it is deduced that the Tibetan Plateau had reached a significant elevation at that time. The late Tertiary palaeoclimatic history of the Red Clay as reflected by magnetic susceptibility is reconstructed during the period of 6.5—2.5 Ma. Stepwise increase in susceptibility of aeolian dust accumulation appears to have a close correlation to the uplift processes of the Tibetan Plateau. The remarkable increase of aeolian dust accumulation at 3.2 Ma appears to be due to the influence of global ice volume on the East Asia monsoon. Palaeomonsoon variation during the late Tertiary as recorded in the Red Clay sequences from the Chinese Loess Plateau can be regarded as the product of a number of interacting factors, such as uplift of the Tibetan Plateau, solar radiation, global ice volume, etc.

Keywords: magnetostratigraphy of Red Clay, aeolian dust accumulation, monsoon variation, uplift of Tibetan Plateau.

The Red Clay strata underlying the Quaternary loess-palaeosol sequences have been widely considered by researchers in China and all over the world for their wide distribution containing mammal fossils. Since the pioneering work of European and Chinese scientists at the beginning of this century, a great deal of work has been carried out on the stratigraphy, pedology, mammal fossil assemblages and the origins of Red Clay in the Loess Plateau. Using the increasing amount of Red Clay data and references, it has been possible over recent years to recognize the aeolian origins of the Red Clay material[1—3]. Therefore, it is clear that aeolian dust accumulation on the Chinese Loess Plateau is not limited to the Pleistocene and Holocene of the last 2.5 Ma. Similarly, it is possible that the East Asia monsoon system that has been controlling the aeolian sequence was developing before the Pleistocene. Meanwhile, it has been demonstrated that the East Asia monsoon system was intrinsically related to the uplift processes of the Tibetan Plateau[4,5]. Thus the importance of the chronostratigraphy and palaeoclimatology of the Red Clay sequences found within the Chinese Loess Plateau is quite clear.

The Red Clay of the Loess Plateau has a thickness of several tens of metres, and contains

* Project supported by the National Natural Science Foundation of China and the Foundation of Xi'an Laboratory of Loess and Quaternary Geology, Chinese Academy of Sciences.

** Also at Institute of Geology, Chinese Academy of Sciences, Beijing 100029, China.

many carbonate layers. On most profiles, interbedded palaeosols and "Red Loess" can be recognized. Pedogenesis of the Red Clay becomes gradually stronger from west to east and from north to south of the Loess Plateau. *Hipparion* fossils have been discovered in the Red Clay strata in many sites over the Loess Plateau[6]. Here we present magnetostratigraphy and palaeoclimate results from the Red Clay sections near Xifeng in the central part of the Loess Plateau and Xi'an in the southern margin of the Loess Plateau. Grain size in Xifeng section shows a single main mode and asymmetric distribution pattern of grain size composition, which is a typical aeolian loess grain size distribution. Similarly, the chemical and mineral composition of the Red Clay is consistent with that of aeolian loess/palaeosols[2]. The data given above provide important evidence to support aeolian genesis of the Red Clay material in many sites of the plateau.

1 Stratigraphy and sampling

The Xifeng Red Clay section (107°27′E, 35°53′N) is located 16 km west of Xifeng City. The Red Clay strata are overlaid by a Quaternary loess-palaeosol sequence and lie on the base of late Tertiary fluvial fine-sand. There is a 1.2 m combination layer between the sand layer and Red Clay. The thickness of Red Clay strata is about 66 m with reddish-light areas, which have only experienced weak pedogenesis. 12 light-red palaeosol complex units with Fe-Mn lamination coating and granulous structure can be recognized over the Red Clay section. Four carbonate layers with a thickness of 0.5—1 m were developed within the lower part of the section. 3 400 powder samples have been collected with sample spacing of 2 cm and 702 oriented palaeomagnetic samples have been collected with sample spacing of 10 cm over the whole Red Clay section.

The Xi'an section is located 5 km east of Xi'an City (109°12′E, 34°12′N). The thickness of Red Clay is nearly 50 m. It underlies the Quaternary loess-palaeosol sequence, and is seated on fluvial sand-gravel. The Red Clay in this section underwent relatively strong pedogenesis, with a light red to deep red colour, containing several tens of layers of carbonate nodules. Mammal fossils of *Hipparion* sp., *Dicorgphochoerus* sp., etc. were discovered within the lower part of the Red Clay strata[7]. Based on previous magnetic stratigraphy work[8], we collected 800 powder samples with sampling space of 4—10 cm for palaeoclimate investigation.

2 Laboratory measurement and data interpretation

Oriented block samples were cut into 2 cm cubes. Two parallel cubes were produced from every sample position for palaeomagnetic measurement. After susceptibility and mass were measured, all samples were demagnetised in an MMTD1 Thermal Demagnetiser made in UK. The samples were subsequently measured using an MINISPIN Magnetometer for Natural Remnant Magnetisation (NRM) from 0 to 600℃ in 40℃ steps. Both the demagnetiser and NRM measurement systems were inside a low magnetic field region. The magnetometer used for NRM measurement has a sensitivity of $10^{-9}Am^2kg^{-1}$. The thermal demagnetizing parameters for NRM measurements are given in table 1.

Table 1 Thermal demagnetisation parameters for Xifeng Red Clay samples

Temperature/℃	0	100	200	260	300	340	420	460	500	600
Heating rate/℃·min^{-1}		100	100	100	100	100	100	100	100	100
Duration/min		10	25	25	30	30	30	30	30	30
Cooling rate/℃·min^{-1}		300	300	300	300	300	300	300	300	300

On the orthogonal diagram of NRM data showing all demagnetisation points, most of the samples have two components from the low to high temperature points. Representative demagnetisation diagrams for normal and reversed samples are shown in fig. 1. Typically the diagrams show the presence of two components. The first is unblocked at low temperatures generally ranging upwards from 0 to 250℃, occasionally reaching 300℃. The direction of this component is consistent with the present-day field, and is thought to be a viscous overprint. On removal of the low-temperature component the direction becomes relatively stable and the vector trends to the origin on the orthogonal plot. This mid-temperature component records a direction corresponding to the palaeomagnetic field when the samples became magnetised.

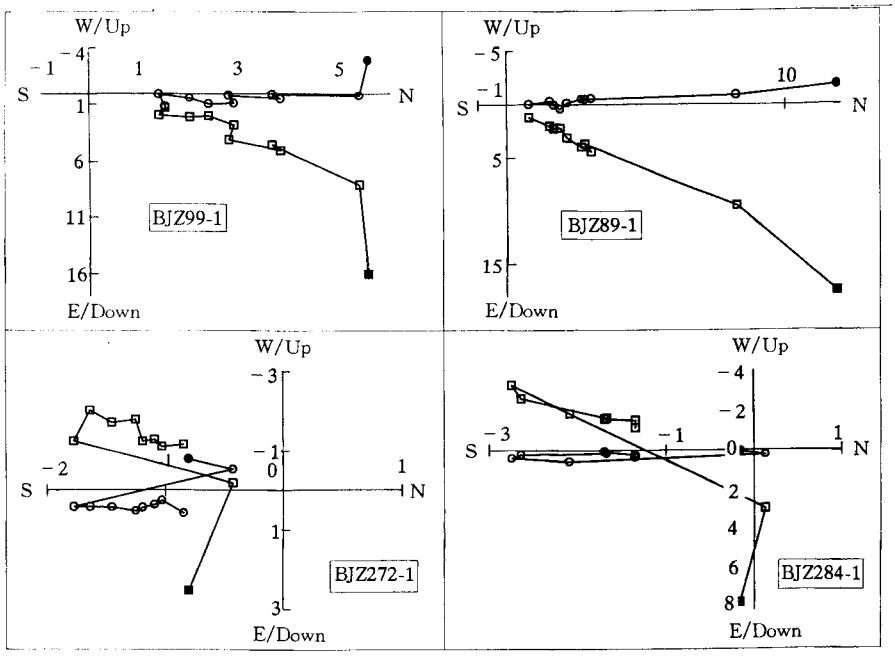

Fig. 1. Orthogonal demagnetisation plots of typical normal and reversed samples of Red Clay in Xifeng. The horizontal component is marked with ○ and the vertical component is marked with □. ● and ■ are room temperature points. The unit of the axes on the plots is $10^{-5}Am^2kg^{-1}$.

3 Results

The stratigraphic column, inclination, declination, and the magnetostratigraphy for the Red Clay section of Xifeng are shown in fig. 2. The magnetochronology of Cande and Kent[9] is shown on the right side of fig. 2, and correlation with our results is very good. We classified the magnetostratigraphy of the Xifeng Red Clay section as follows. The top 3.2 m of the section shows negative polarity and belongs to the Mutuyama Chron. 3.2—32.02 m is normal polarity and belongs to the Gauss Chron, within which the two reversed polarity events correspond to the Kaena and Mammoth events respectively. The next reversed polarity section at 32.02—56.8 m is the Gilbert Chron. There are just 4 normal polarity events, which is consistent with the magnetochronology of Cande and Kent. The normal polarity at 56.8—61.82 m corresponds to 3An.1n. It seems that the normal polarity seen at 64.43—65.29 m is relatively thin when we correlated it

to Chron3An.2n. We believe that the above correlation is correct because the sedimentation rate through the 64.63—65.29 m strata is probably different from the Red Clay above it as it is in the transition layer between normal Red Clay and fluvial sand. The global geomagnetic time scale before 6.0 Ma shows significant differences between investigations[9,10]. In the Red Clay section we temporarily correlate 64.63—65.7 m normal polarity to 3An.2n. Using the magnetostratigraphy of the whole section we can determine the boundary ages of the magnetic reversal, which can be used as the controlling age points for the time scale of the Red Clay sequence. Subsequently the time scale can be obtained by linear interpolation between age points. Similarly, the top and the bottom ages of the Red Clay strata can be calculated by extrapolation using the accumulation rate of the strata near the top or bottom layer of the Red Clay. In this way, the time scale of the Red Clay stratigraphy can be obtained. The basal age of the Red Clay strata of the Xifeng section is 6.6 Ma.

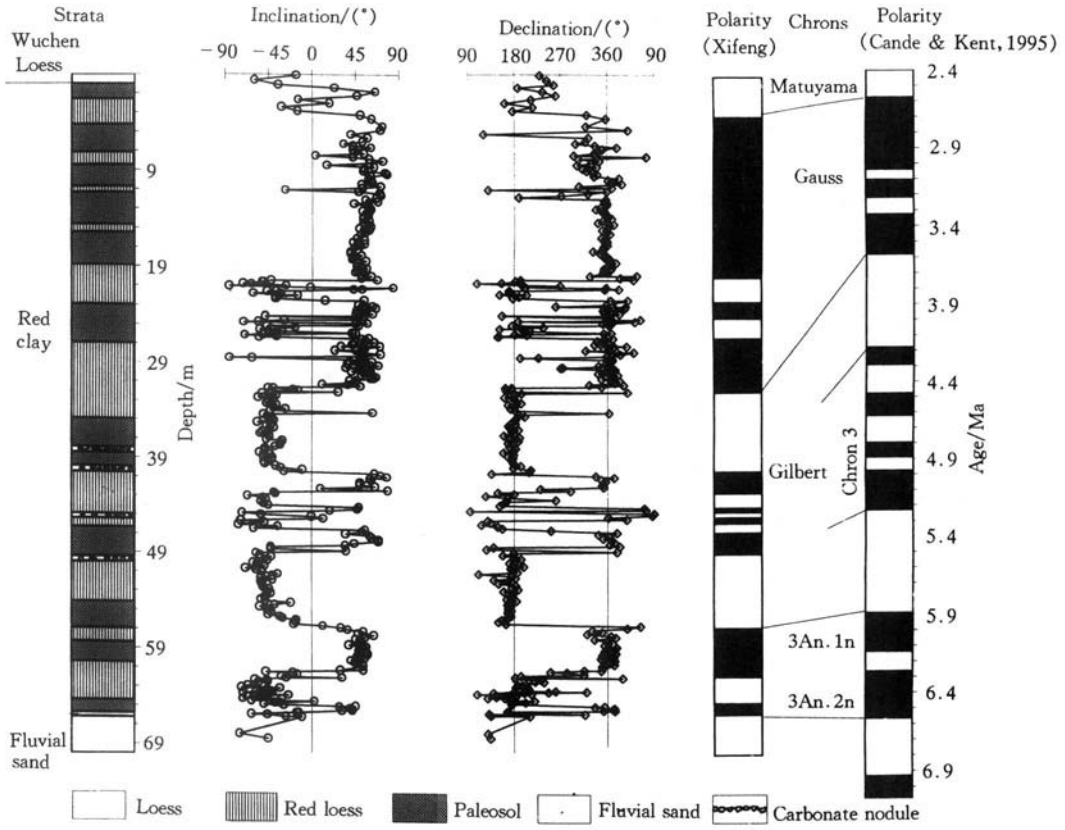

Fig. 2. Stratigraphic column, magnetic polarity column, declination, inclination and the magnetic reversal time scale of the world. Black columns in the figure represent normal polarity and white reversed one.

Based on the previous palaeomagnetic data[8] we made some modification to the magnetostratigraphy of the Xi'an section. In our magnetic polarity transition investigation of the section, we position the G/M boundary at 1.48 m below the Red Clay/Loess boundary. Although only two normal events were marked on the strata between 22 and 32 m on the original polarity column, the original declination and inclination data actually show some shifts. Therefore,

according to theaccumulation rate of the strata the 22—32 m reversal should be correlated to Chron3n. Correspondingly, the normal polarity of 36—42.5 m is correlated to Chron 3An. The same technique was used to set up a time scale for the Xi'an Red Clay strata, which gives the bottom age of the Red Clays as 6.8 Ma. This is close to that of Xifeng.

Aeolian dust accumulation rate of the last 6.5 Ma in the Xifeng area can be determined when the magnetostratigraphy of the Quaternary aeolian loess-palaeosol sequence[11] is compiled together with the Red Clay sequence. The result shows that the aeolian accumulation rate obviously increases at 3.2 Ma B.P.

The susceptibility curve from Xifeng is similar to that of the Xi'an section, but the Red Clay sequence in Xifeng has a higher resolution and weaker pedogenesis than at Xi'an (fig. 3) because Xi'an is located in the southern margin of the Loess Plateau. Therefore the Xifeng section provides a reliable high-resolution palaeomagnetic and palaeoclimatic record. Susceptibility values from Xifeng are within the range of 20—120 units (10—8 m^3/kg). There are 6 high value peak zones at depths of 12, 24, 37, 48, 60, and 65 m, which correspond to palaeosol complexes within the profile. Susceptibility of the underlying fluvial sand is lower than 10 units. The Xi'an section shows susceptibility variations of 30—150 units, which is higher than the corresponding layer of the Xifeng section.

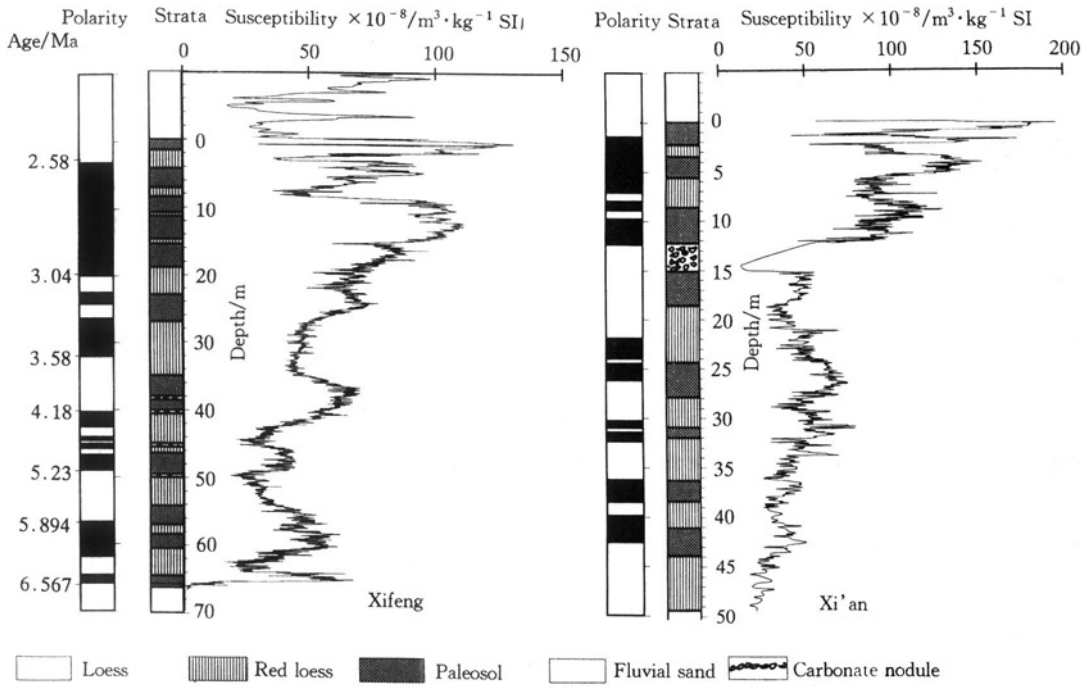

Fig. 3. Magnetic susceptibility curves for the Red Clays of the Xifeng and Xi'an sections.

4 Discussion

(1) It has been demonstrated that the Quaternary loess-palaeosol sequence of the Loess Plateau is the product of the east Asia monsoon variation and that magnetic susceptibility is interpreted as the proxy index of summer monsoon, while aeolian accumulation rate and grain size of

the aeolian dust reflects the aridity of the source area, and is, therefore, an indicator of the strength of the winter monsoon[1]. Similarly the magnetic susceptibility and the aeolian dust accumulation rate of the Red Clay sequence consisting of alternating reddish loess and reddish palaeosol (Red Clay) is controlled by the winter and summer monsoon variation of the Loess Plateau during the late Tertiary. Our results suggest that the aeolian dust accumulation and the East Asia palaeomonsoon began to develop at least 6.5 Ma ago. Considering the suggestion that the development of the East Asia palaeomonsoon and the start of aeolian dust accumulation over the Loess Plateau were intrinsically related to the uplift of the Tibetan Plateau[5], it can be deduced that the Tibetan Plateau had reached sufficient elevation to modify the atmospheric circulation of East Asia at 6.5 Ma B.P. This is confirmed by the India monsoon record[12].

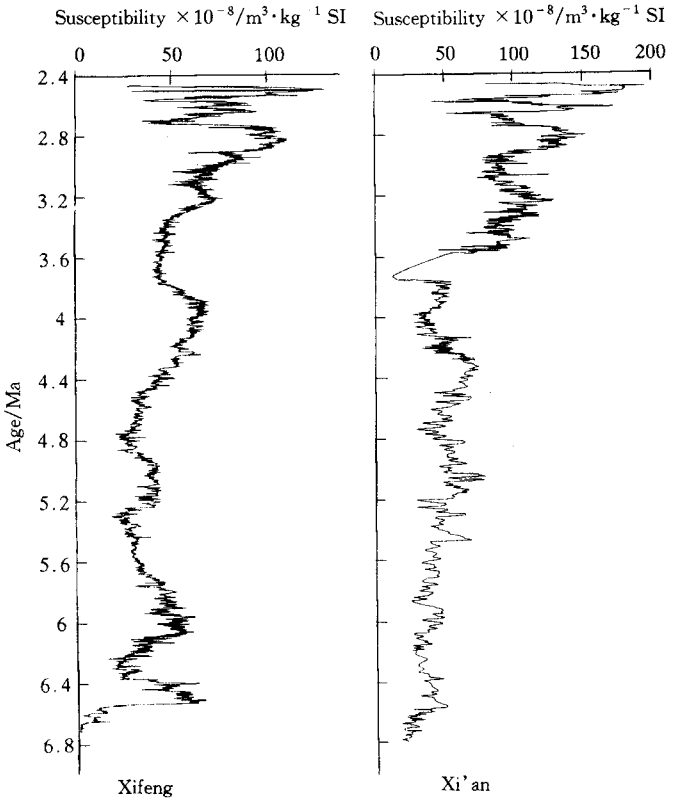

Fig. 4. Time series sequence of the proxy climatic index of susceptibility of the Xi'an and Xifeng sections.

(2) It can be seen from fig. 4 that the susceptibility value increased stepwise from the bottom to the top of the Red Clay sequence. The strengthening of the summer monsoon indicated by susceptibility curves occurred at 5.4, 4.4, 3.4, 2.4 Ma. There are six high susceptibility value zones corresponding to palaeosol complexes which represent strengthened summer monsoon periods. They are dated at 6.5, 6.0, 5.0, 4.0, 3.3 and 2.8 Ma, of which 2.8 Ma and 3.3 Ma are the two strongest summer periods, probably representing climatic optima of the late Tertiary. Climatic fluctuation reflected by susceptibility curves show a strong 1 Ma quasi-cycle. This quasi-cycle coincides with the tectonic cycle of the Tibetan uplift demonstrated by Wu *et al.*[5], which reveals the controlling role of the Tibetan Plateau on the East Asian monsoon and aeolian dust process over the Loess Plateau as well as the East Asian continent. Stepwise increase of susceptibility value may reflect the stepwise uplift process of the Tibetan Plateau.

(3) Statistical counting of the susceptibility curves shows the existence of quasi 20 ka, quasi 40 ka cycles and quasi 2 Ma in the climatic fluctuation of the late Tertiary Red Clay. This result suggests that the solar insulation resulting from the orbital changes of the Earth played an important role in the East Asia monsoon variation even as early as the late Tertiary.

(4) The aeolian dust accumulation rate obviously increased at 3.2 Ma B.P. over the last 6.5 Ma. This is interpreted as the result of the growth of the global ice volume at that time[13],

particularly the Northern Hemisphere, showing the influence of the global ice volume on the East Asian monsoon and aeolian dust accumulations on the Chinese Loess Plateau.

Therefore, palaeomonsoon variation in the late Tertiary recorded in aeolian Red Clay sequences of the Chinese Loess Plateau can be regarded as the product of interactions between the uplift process of the Tibetan Plateau, solar insulation variation, and global ice volume changes.

Acknowledgement We thank Sun Yubin, Nai Zhongping, Lu Huyu, Su Zhiheng and Zhou Fei for their help in field work and sample measurements. We also express our special thanks to Prof. Wu Xihao for his help during writing this paper.

References

1 An Zhisheng, Wu Xihao, Wang Pingxian *et al.*, Paleomonsoon of China over the last 130 ka——Ⅱ. Paleomonsoon variation, *Science in China* (in Chinese), Ser. B, 1991, (11): 1209.

2 Zhao Jinpo, Research on the later Tertiary Red Clay in Xi'an and Baode, *Acta of Sedimentology* (in Chinese), 1989, 7: 113.

3 Yuan Baoyin, Developing mechanism and its evolution process of the loess geomorphology in China, in *Geomorphology in China and Its Evolution* (in Chinese), Beijing: China Ocean Press, 1993, 132—148.

4 Ye Duzheng, Gao Youxi, *Meteorology of Tibetan Plateau* (in Chinese), Beijing: Science Press, 1979, 1—257.

5 Wu Xihao, Wang Fubao, An Zhisheng *et al.*, Uplift stage and elevation of Tibetan Plateau over the Late Cenozoic, in *Loess · Quaternary Geology · Global Change*(3) (eds. Liu Tungsheng, An Zhisheng) (in Chinese), Beijing: Science Press, 1992, 1—13.

6 Qiu Zhangxiang, Huang Weilong, Gao Zhihui, *Hipparion Fossil in China* (in Chinese), Beijing: Science Press, 1987, 1—250.

7 Jia Lanpo, Zhang Yuping, Huang Wanpo *et al.*, Cenozoic stratigraphy of Lantian area, Shaanxi Province, in *Proceeding Conference Cenozoic of Lantian Area, Shaanxi Province*, Beijing: Science Press, 1966, 1—31.

8 Zheng Hongbo, An Zhisheng, Shaw, J. *et al.*, Study on magnetostratigraphy of Duanjiapo loess profile, in *Loess · Quaternary Geology · Global Change*(3) (eds. Liu Tungsheng, An Zhisheng) (in Chinese), Beijing: Science Press, 1992, 38—43.

9 Cande, S.C., Kent, D.V., Revised calibration of the geomagnetic polarity timescale for the late Cretaceous and Cenozoic, *Journal of Geophysical Research*, 1995, 100: 6093.

10 Baksi, A.K., Fine tuning the radiometrically derived geomagnetic polarity time scale (GPTS) for 0—10 Ma, *Geophysical Research Letters*, 1995, 22: 457.

11 Liu, X.M., Liu, T.S., Xu, T.C. *et al.*, The primary study on magnetostratigraphy of the Loess Profile in Xifeng area, Gansu Province, *Geophy. F. R. Astr. Soc.*, 1988, 92: 345.

12 Prell, W.L., Kutzbach, J.R., Sensitivity of the Indian monsoon to forcing parameters and implications for its evolution, *Nature*, 1992, 360: 647.

13 Shackleton, N.J., Hall, M.A., Pate, D., Pliocene stable isotope stratigraphy of site 846, in *Proceedings of the Ocean Drilling Program, Scientific Results* (eds. Pisias, N.G., Mayer, L.A., Janecek, T.R. *et al.*), Texas: College Station, 1995, 138: 337—355.